Marine Geology 480 (2025) 107471

Contents lists available at ScienceDirect

Marine Geology

journal homepage: www.elsevier.com/locate/margo

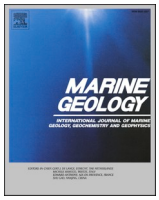

Research Article

Evaluating longshore sediment transport: A comparison between empirical formulas and XBeach 2DH numerical model

Samanta Buttò [a,b,*], Carla Lucia Faraci [c], Marta Corradino [a], Claudio Iuppa [c], Emanuele Colica [d], Fabrizio Pepe [a]

[a] Department of Earth and Marine Sciences (DiSTeM), University of Palermo, Via Archirafi 22, 90123 Palermo, Italy
[b] Department of Biological, Geological and Environmental Sciences (DBGES)– Earth Sciences Section, University of Catania, Corso Italia 57, 95129 Catania, Italy
[c] Department of Engineering, University of Messina, Contrada di Dio, Sant'Agata, 98166 Messina, Italy
[d] Department of Geosciences, University of Malta, Msida, MSD 2080, Malta

ARTICLE INFO

Editor: Shu Gao

Keywords:
Longshore sediment transport
Coastal erosion
Empirical formulas
XBeach 2DH numerical model

ABSTRACT

Longshore sediment transport (LST) is a crucial process shaping coastal environments. As multiple site-specific factors (e.g. wave height, coastal topography) influence the LST, an accurate estimation of LST rate represents a scientific challenge.

This research evaluates the predictive capacity of three widely used empirical formulas (CERC, 1984; Kamphuis, 1991; Van Rijn, 2014) and the XBeach 2DH numerical model for estimating the LST rate by comparing the obtained results with field LST data.

We chose three coastal sites in Malta Island (Għadira Bay, GB) and northern Sicily (Cefalù, CF, and Campofelice di Roccella, CR) based on different sediment grain size, coastal type (open or embayed) and morpho-bathymetry.

For each site, we analysed wave parameters, grain size of the beach and seabed sediments, coastal morphology, and marine vegetation distribution. Furthermore, we used field measurements to calibrate the numerical model's sediment transport and morphological parameters.

The calibrated numerical model provides greater accuracy in LST rate estimation than the empirical formulas. The latter overestimates the LST rates by factors ranging from 435 to 7885, whereas the numerical model overestimates by factors of 1.8 and 1.9 at the CF site and GB, respectively, and underestimates by a factor of 0.5 at the CR site.

The good performance of the numerical model is due to its consideration of site-specific factors. The parameter values for the model calibration can be used successfully in embayed fine/coarse sandy beaches. Moreover, the numerical model, tested so far only for sandy beaches, also works well on gravelly beaches.

1. Introduction

Longshore sediment transport (LST) is a natural process that influences the dynamics and evolution of coastal environments. Various factors, including the site's sedimentological, morphological, and biotic components, significantly determine the LST rate (Pereira Quadrado and Goulart, 2020; Salem Cherif et al., 2019; Widdows and Brinsley, 2002). In embayed systems, the bathymetry of the inner shelf (Dolique and Anthony, 2005) and the dimensions of the headlands (King et al., 2021) influence sediment retention even under conditions of strong currents and waves (Dehouck et al., 2009). Whereas vegetation on the seabed reduces the shear stress at the sediment-water interface and, thus, the sediment erosion (Le Hir et al., 2007; Widdows and Brinsley, 2002).

The main approaches for estimating LST rate are empirical formulas and numerical models. Empirical formulas, such as bulk transport formulas, represent physical processes through explicit equations based on readily available input parameters (e.g., wave height and water depth at the breaking point, wave period, breaking wave angle, median sediment grain size, seabed slope, water, and sediment density) and empirical coefficients (Bailard, 1981; Bayram et al., 2007; Walton et al., 1989). However, most formulas were unsuccessful because they include weakly defined parameters (e.g. beach slope) or are based on a limited data set

* Corresponding author at: Department of Earth and Marine Sciences (DiSTeM), University of Palermo, Via Archirafi 22, 90123 Palermo, Italy.
E-mail address: samanta.butto@unipa.it (S. Buttò).

https://doi.org/10.1016/j.margeo.2024.107471
Received 24 October 2024; Received in revised form 23 December 2024; Accepted 27 December 2024
Available online 29 December 2024

(e.g., range of grain size or wave heights). Moreover, bulk formulas are calibrated with empirical coefficients that depend on field data, so their accuracy is linked to the quality of field measurements or the specificity of the survey site.

Various formulas exist for calculating LST, differentiated by the variables they depend on, such as sediment grain size, seabed slope, wave period or water depth at breaking point. Among these, the CERC formula (1984) and Kamphuis's (1991) formula are widely used in both practice and fundamental research. Many researchers focused on calibration of the parameters that influence the LST rate value to improve the formulas' accuracy (Bodge and Kraus, 1991; Eversole and Fletcher, 2003; Mil-Homens et al., 2013; Pereira Quadrado and Goulart, 2020; Salem Cherif et al., 2019; Sanil Kumar et al., 2003; Shanas and Sanil Kumar, 2014; Wang et al., 1998, 2002; Williams et al., 2008). For instance, Mil-Homens et al. (2013) used the least-squares optimization algorithm to calculate a coefficient relating sand transport to longshore energy flux in the CERC (1984) formula and a series of parameters of the Kamphuis (1991) formula. Other authors have attempted to refine the CERC (1984) formula, by revising the k parameter value (Bodge and Kraus, 1991; del Valle et al., 1993; Eversole and Fletcher, 2003; Schoonees and Theron, 1993; Van Wellen et al., 2000), and the Kamphuis (1991) formula, by calibrating the exponent of the median diameter (D50) to modify the weight of the grain size parameter (Mil-Homens et al., 2013; Tomasicchio et al., 1994; Tomasicchio et al., 2013; Van Rijn, 2014). Also, Van Rijn (2014) analysed the research of CERC (1984), Kamphuis (1991), and Mil-Homens et al. (2013) and proposed a general and dimensionally correct predictive formula.

Numerical models simulate the hydrodynamic processes of short-wave transformation (refraction, shoaling, and breaking) and long-wave transformation (generation, propagation, and dissipation) and compute sediment transport (both suspended and bed total load) and morphological changes (Delft3D of Lesser et al., 2004, MIKE21 of DHI, 2005 and UNIBEST of WL|Delft Hydraulics, 1994). Previous studies used numerical models for the LST estimation in different coastal environments, e.g. gravel beaches (Tomasicchio et al., 2017), fine-grained to coarse-grained sand beaches (Haas and Hanes, 2004; Williams et al., 2008), sand and gravel/shingle beaches (Van Rijn, 2003).

The numerical models estimate LST by solving the fundamental fluid motion equations, such as the Navier-Stokes equations for incompressible flow, the shallow water equations for wave propagation, and the advection-diffusion equation for sediment transport. The models use numerical methods like finite difference or finite element techniques to solve these equations, allowing them to calculate key parameters influencing sediment transport, such as wave breaking, radiation stresses, turbulence, bed shear stress, equilibrium sediment concentration, and flow velocity.

Models differ for the spatial dimensions of the phenomenon (Samaras and Koutitas, 2014). One-dimensional (1D) models (e.g. GENESIS of Hanson (1989), ONELINE of Dabees and Kamphuis (1998) and SMC of González et al. (2007)) study sediment transport along a single cross-shore transect. Two-dimensional (2D) models (e.g. Dally–Dean model of Dally and Dean (1984), UNIBEST of Roelvink and Stive (1989), LITCROSS of Hedegaard et al. (1991) and XBeach of Roelvink et al. (2009)) analysed the transport process in a plane by using horizontal (2DH) or vertical (2DV) computational grids. Three-dimensional (3D) models (e.g. CH3D-SED of Gessler et al. (1999), Delft3D of Lesser et al. (2004) and GAIA-TELEMAC of Tassi et al. (2023)) integrate a sediment transport model with a hydrodynamics model to solve equations of continuity and motion over a 3D grid.

The modelling approach is more labour-intensive than the application of formulas due to its reliance on relatively detailed and numerous input data. Moreover, the model complexity frequently requires a site-specific calibration based on field data to improve the result accuracy (Bergillos et al., 2017; Elsayed and Oumeraci, 2017; Garzon et al., 2022; Hwang et al., 2024; Jin et al., 2021; McCall et al., 2010; Satheeshkumar and Balaji, 2021; Simmons et al., 2019; Simmons and Splinter, 2022). Following several studies, the calibration process should consider sediment transport parameters and morphology parameters because they are the most influent on the LST rate (Bugajny et al., 2013; Elsayed and Oumeraci, 2017; Hwang et al., 2024; Satheeshkumar and Balaji, 2021).

2D models reach a satisfactory balance between result accuracy and computational time compared with 1D and 3D models. In particular, the 2DH numerical models are the most suitable for predicting LST rate because they consider 1) the areal morphological and hydrodynamics variability of the site compared to 1D models and 2) alongshore variations of water levels, fluid velocities and their derivatives compared to 2DV models. Despite continuous efforts to refine the LST estimation methods, an open problem regards the accuracy of the methods used in different coastal environments. This study aims to evaluate the predictive capacity of three of the most commonly used bulk formulas: the CERC formula (1984), the Kamphuis formula (1991) and the Van Rijn formula (2014). These formulas are compared to the XBeach 2DH numerical model (Roelvink et al., 2009) for estimating the LST rate under non-extreme conditions. The research defines which approach provides the most accurate LST value for different coastal settings by comparing the results of the empirical formulas and the numerical model with field-acquired LST data. Furthermore, the influence of seabed vegetation on the LST rate is investigated.

The coastal areas of Għadira Bay (GB, Malta Island), Cefalù (CF, northern Sicily), and Campofelice di Roccella (CR, northern Sicily) were selected for this study due to their distinct characteristics, including beach sediment grain size, coastal type (open or embayed system), seabed morphology, and presence of vegetation.

This research highlights the importance of selecting a LST estimation method based on site-specific characteristics. An accurate estimate of the LST value is essential for effective coastal management, erosion mitigation, and the preservation of coastal ecosystems.

The paper is organized as follows: Section 2 presents the study areas; Section 3 describes the materials and methods used to collect and analyse data (field measurements and wave parameters) and to calculate the LST rate (bulk formulas and XBeach 2DH model); Section 4 outlines the results of the morphologic and granulometric analysis of the sites, wave conditions, marine vegetation, LST rate value for each site; Section 5 discusses the bulk formulas and XBeach 2DH model's results and compares them with field observations; Section 6 highlights the conclusion of this research.

2. Oceanographic and climatic conditions of the study areas

2.1. Malta Island

Malta Island is located in the central Mediterranean Sea, approximately 100 km south of Sicily (Fig. 1 a). Its coastal climate is subjected to the dynamics of air pressure systems originating from the Atlantic and nearby landmasses. The storms affect the island principally during autumn and winter, driven by the convergence of low-pressure systems with warm, moist air over the Mediterranean (Galdies, 2011). A twenty-nine-year observation period reveals a mean annual surface wind speed of 16.3 km/h, with prevailing north-westerly winds dominating 20.7 % of days annually (Galdies, 2011). The winds significantly shape wave patterns around the islands. The analysis of a fourteen-year dataset by the Malta Maritime Authority (MMA, 2003) indicates similar directions of offshore waves and winds, suggesting that local wind-generated waves play a more significant role than swell waves.

The wave climate has a strong seasonal energy pattern, with peak energy concentrated during the winter months from November to April (Drago et al., 2013). The annual mean significant wave height ($H_{s,m}$) is 1.22 m, increasing to 1.92 m during winter (Drago et al., 2013).

We selected the beach of GB as a study area for this research. The GB site is an embayed system located in the northeast sector of the island (Fig. 1 a and e) and bounded by headlands on both sides. The beach consists of about 5 m thick sandy barrier that borders salt marshes and

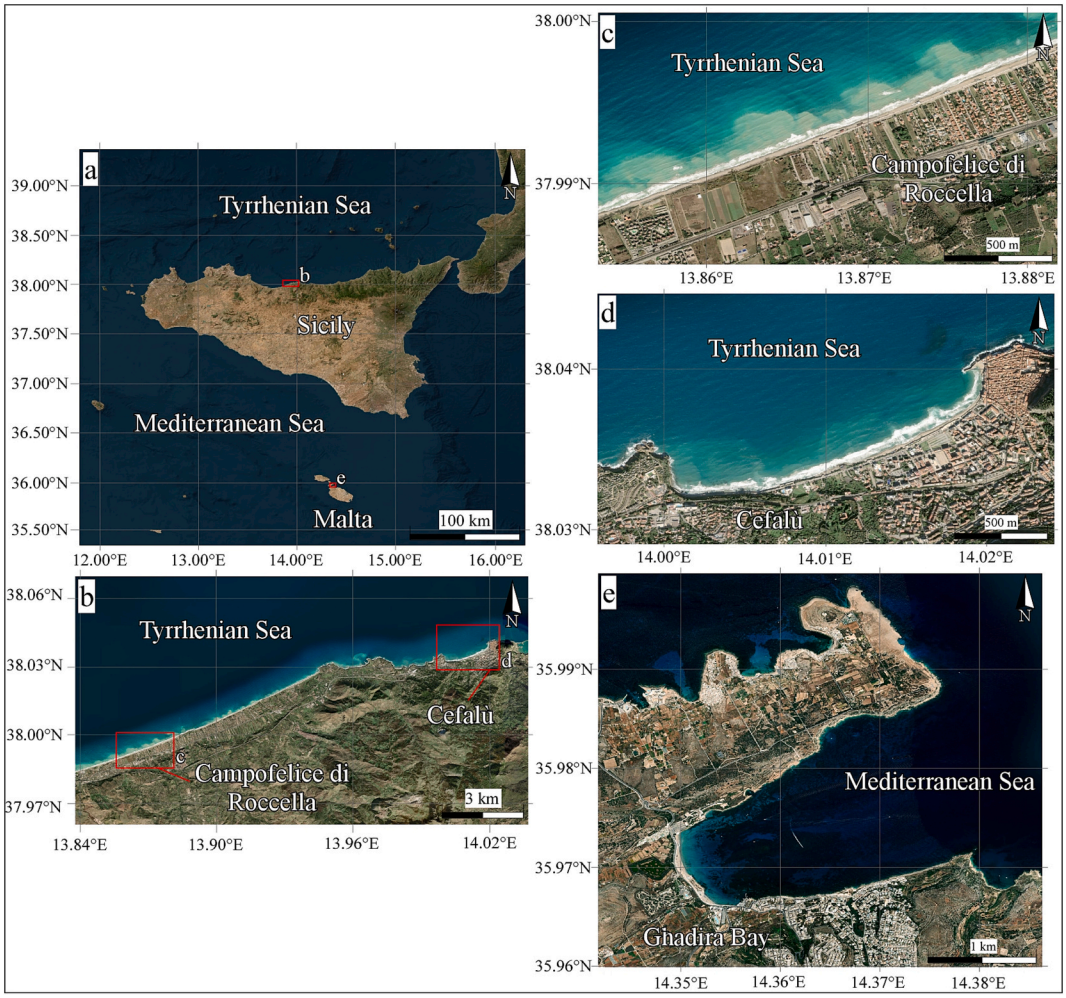

Fig. 1. (a) Geographic locations of the study areas: (b) northern Sicily, featuring the sites of (c) Campofelice di Roccella and (d) Cefalù; (e) Għadira Bay on Malta Island.

pools (Gatt, 2021). An observation period between 12:00 am on 1st January 1993 and 11:00 pm on 31st December 2023 revealed that north-westerly waves are predominant at GB site, with significant wave height (H_s) typically between 0.5 and 1 m, and frequencies of about 15 % (Fig. 2c).

2.2. Northern sicily

The northern coast of Sicily is located in the southern Tyrrhenian Sea (Fig. 1 a and b). The wind climate of this area is characterized by seasonal variability, including the southwest Libeccio wind in winter, the southeast Sirocco wind in autumn and spring, and the north-northwest Mistral wind, typically in winter (Barbariol et al., 2021). Also, this area is characterized by winds with the highest speed variability of the Mediterranean basin during the year (Soukissian et al., 2018). In the observation period between 2015 and 2019, the maximum value of mean annual surface wind speed was about 15 m/s, with a north-northwestern direction and occurrence frequency greater than 14 % (Sperati et al., 2024; https://atlanteeolico.rse-web.it/).

The wave climate is mainly controlled by regional winds and the morphological complexity of the offshore areas, resulting in limited fetches in coastal shallow regions relatively proximal to the generation areas (Barbariol et al., 2021). The trend analysis of the wave time series over 40 years shows that the highest wave power values occur during winter, in agreement with the increase of H_s in the same period (Caloiero et al., 2022).

Along the northern coast of Sicily (Fig. 1 b), we selected two study areas, the CR (Fig. 1 c) and CF sites (Fig. 1 d). The CR site is an open system characterized by a 1.5 km long and 40 m wide gravel beach. Meanwhile, the CF site is an embayed system bounded by headlands on both sides. This site consists of a sandy beach, approximately 1.7 km long, limited landward by anthropic structures. An observation period from 12:00 am on 1st January 1993 to 11:00 pm on 31st December 2023 revealed that sites CR and CF are predominantly affected by waves from the northwest, with H_s typically ranging between 0.5 and 1 m, occasionally exceeding 2 m (Fig. 2 a and b).

3. Materials and methods

3.1. Data collection

3.1.1. Digital elevation models and seafloor mapping

Digital Elevation Models (DEMs) of the emerged coastal areas of CR and CF sites were derived from LIDAR data with a resolution of 2 m, acquired during ATA flights in 2012/2013, available in the SITR portal of the Sicily Region (https://map.sitr.regione.sicilia.it/gis/services/modelli_digitali/mdt_2013/ImageServer/WCSServer). DEM of the emerged coastal area of the GB site was obtained by aerial photogrammetric data acquired by an unmanned aerial vehicle (UAV) Mavic 3 Enterprise and processed using Agisoft Metashape v. 2.0.0. The photogrammetric data were also used for the mapping of *Posidonia oceanica* in the area extending from the coastline to 10 m of depth. The map of

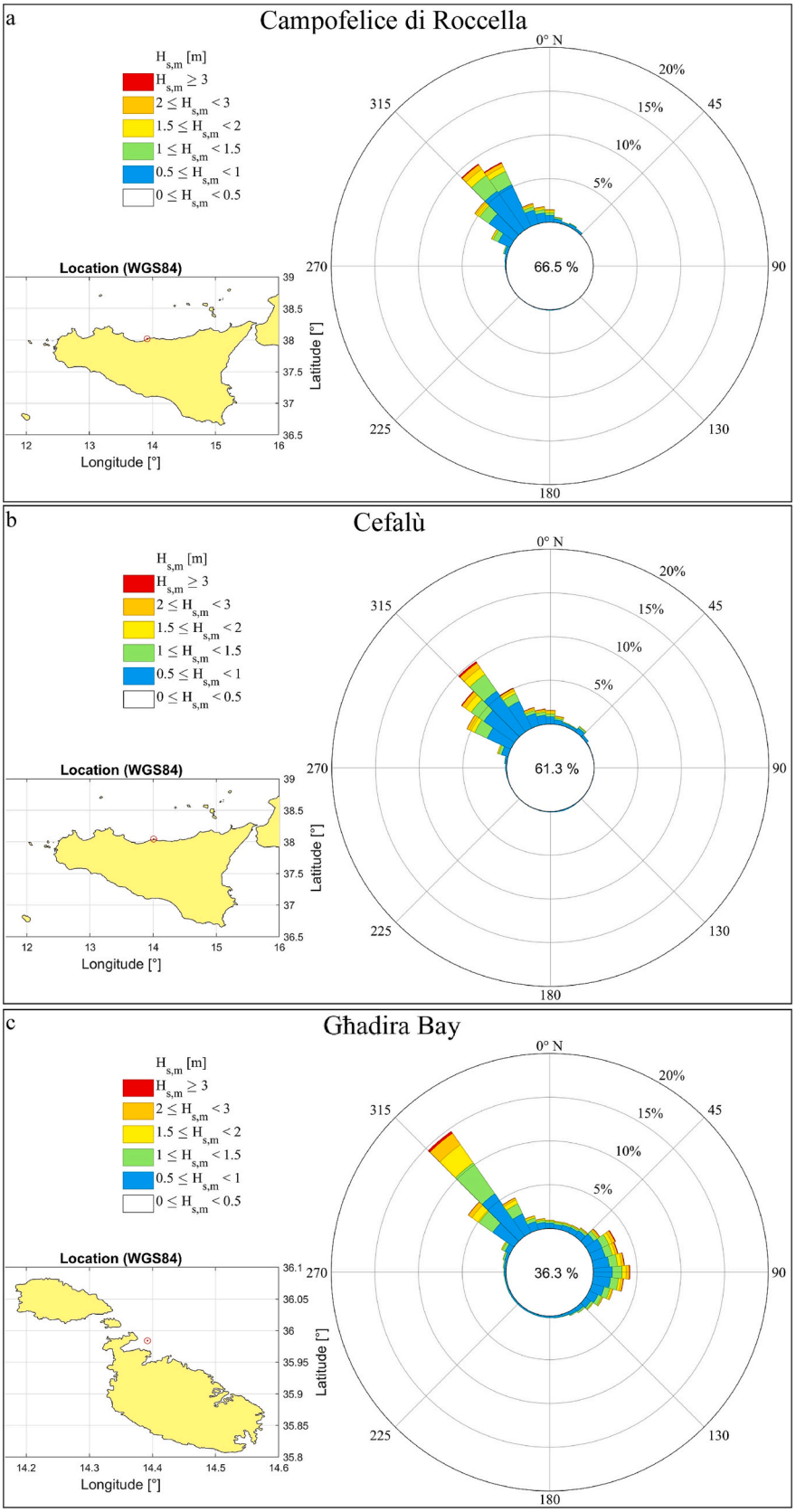

Fig. 2. Wave rose of annual mean significant wave height and direction at the sites a) Campofelice di Roccella, b) Cefalù and c) Għadira Bay, for the period between 12:00 am on 1st January 1993 and 11:00 pm on 31st December 2023. The red points in the maps indicate the offshore points where wave parameters have been downloaded from the Copernicus Marine Service Information. (For interpretation of the references to colour in this figure legend, the reader is referred to the web version of this article.)

P. oceanica distribution was created by using QGIS software.

Bathymetric data from zero to approximately 20 m of depth were obtained at all three sites (CR, CF, and GB) using a 235 kHz Ohmex SonarMite V5 single beam echo-sounder mounted on a small inflatable boat. These data were integrated with Topcon Hyper HR GNSS data collected in the surf zone (depth range 0–1.5 m). The bathymetric maps were generated by processing the single beam and GNSS data using SAGA GIS software and applying the linear ordinary Kriging interpolation method.

3.1.2. LST rate measurement

A "streamer trap" was built based on the model proposed by Kraus (1987) to collect data on LST rates in the surf zone. The instrument consists of four rectangular collection bags, called streamers, that allow the capturing of sediment both at the seabed and in suspension (Fig. 3 a). The streamer's mouth is 20 cm wide and 16 cm high. The bags are made of polyester-sieve cloth with a 60 μm mesh size to trap sand to gravel size sediment. The streamers were vertically mounted on a metal frame: the lowest streamer and the uppermost one were positioned 2 cm and 75 cm from the seabed, respectively. Streamer traps have several limitations that can cause errors in the measurements. One of the significant limitations is the need for continuous controls of bags that tend to wrap around the legs of the rack if the current is weak or intermittent due to oscillatory water motion caused by the passage of waves (Kraus, 1987). Another difficulty is using the streamer traps for wave-breaking heights of more than 1 m due to their manual deployment and the possibility that the trap tips in the direction of forward wave motion (Kraus, 1987). Moreover, streamer traps are susceptible to both oversampling and undersampling issues. The oversampling can be due to the stirring of sediments when the trap is positioned at the seabed. The undersampling may result from 1) the gap between the seabed and the first bag, as well as between the trap's bags, which do not allow the capture of all sediments moving along the seabed and in suspension in the water column; 2) the trap structure that partly obstructs the seabed load transport (Masselink et al., 2009).

Acquisition surveys were carried out in the study areas on 27th July 2023 (CR site), 24th January 2024 (GB site), and 2nd April 2024 (CF site, Fig. 3 b). The LST field measurements are generally affected by errors due to random variables such as instrumental limitations (described above) and wave climate variability during sampling. To reduce the error bar of the field measurements, we followed the acquisition procedure proposed by Kraus (1987) and adopted in subsequent studies (e.g. Cartier and Héquette, 2015; Williams et al., 2008). The measurements lasted 10 min to minimise 1) disturbances to the bottom flow caused by the presence of the trap (Cartier and Héquette, 2015; Kraus, 1987; Pereira Quadrado and Goulart, 2020; Williams et al., 2008) and 2) errors due to variability in wave climate, as the wave properties are considered steady for a sea state of a hundred of waves (i.e. of timespan of the order of 1 h, Boccotti, 1997). Field measurements of LST were repeated twice at each site to improve the data robustness and to estimate error bars.

The LST rate (Q_t) was determined by the approach proposed by Kraus (1987) and modified by Wang et al. (1998):

$$F_k = \frac{m_s}{t}$$

$$\Delta F_k = \left(\frac{\frac{F_{k+1}}{h_{k+1}} + \frac{F_{k-1}}{h_{k-1}}}{2} \right) * \Delta z_k$$

$$Q_t = \sum_{k=1}^{n} F_k + \sum_{k=1}^{n-1} \Delta F_k$$

Where F_k is the sediment flux at streamer k (kg/s), m_s is the mass of sand at streamer k (kg), t is the sample time (s), ΔF_k is the sediment flux between two adjacent streamers (kg/s), F_{k+1} and F_{k-1} are the fluxes through the upper and lower streamers (kg/s), h_{k+1} and h_{k-1} are the vertical widths of the opening of the upper and lower streamers (m), Δz_k is the distance between two adjacent streamers (m) and n is the number of streamers mounted on the trap.

3.1.3. Granulometric data

Sediment samples were collected along the study areas' beach face and surf zone seabed. The sediment grain size was determined using the ASTM international standard method (D422–63 and D2217–85) with eight sieves spaced from 8 mm to 63 μm. Median diameter (D50) and 90 % diameter (D90) were extracted by following geometric graphical measures (Folk and Ward, 1957) using Gradistat software (Blott and Pye, 2001). Additionally, granulometric curves were elaborated for CR, CF, and GB sites.

3.1.4. Wave data

The wave parameters were downloaded from Copernicus Marine Service Information. In particular, we used data from the product "Mediterranean Sea Waves Analysis and Forecast" (Korres et al., 2023). The variables include offshore significant wave height (H_o), wave period at spectral peak (T_p), and mean direction of the wave from (D_{ir}). We used a 12-h time series of wave parameters for each day in which we carried out the LST measurements (Fig. 4 a, b and c). Only for the GB site, we also considered the significant wave height (H_b), the wave period at spectral peak ($T_{p,br}$) and the mean direction ($D_{ir,br}$) at the breaking

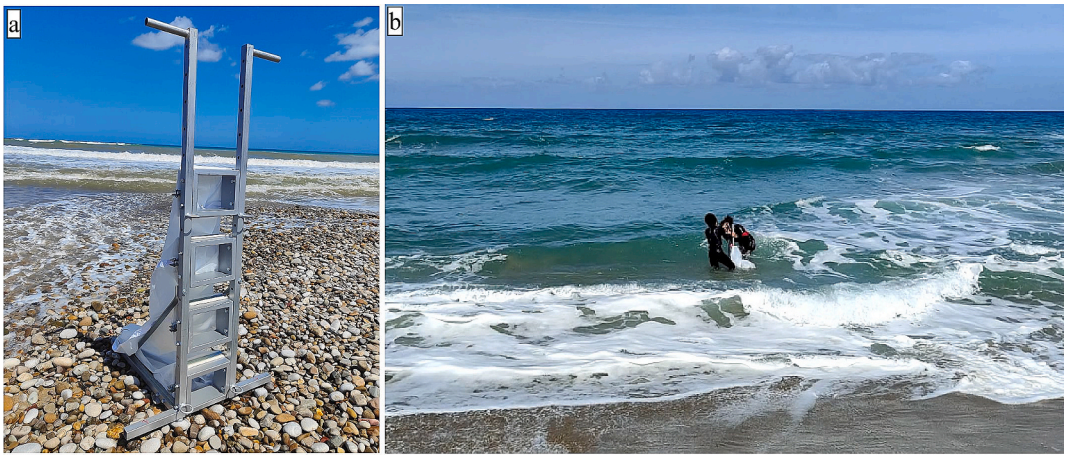

Fig. 3. (a) Streamer trap used to measure field LST rate. b) Example of acquisition survey at the Cefalù Site performed on 2nd April 2024 with a significant offshore wave height of 0.6 m, direction 297°N and period of 8 s.

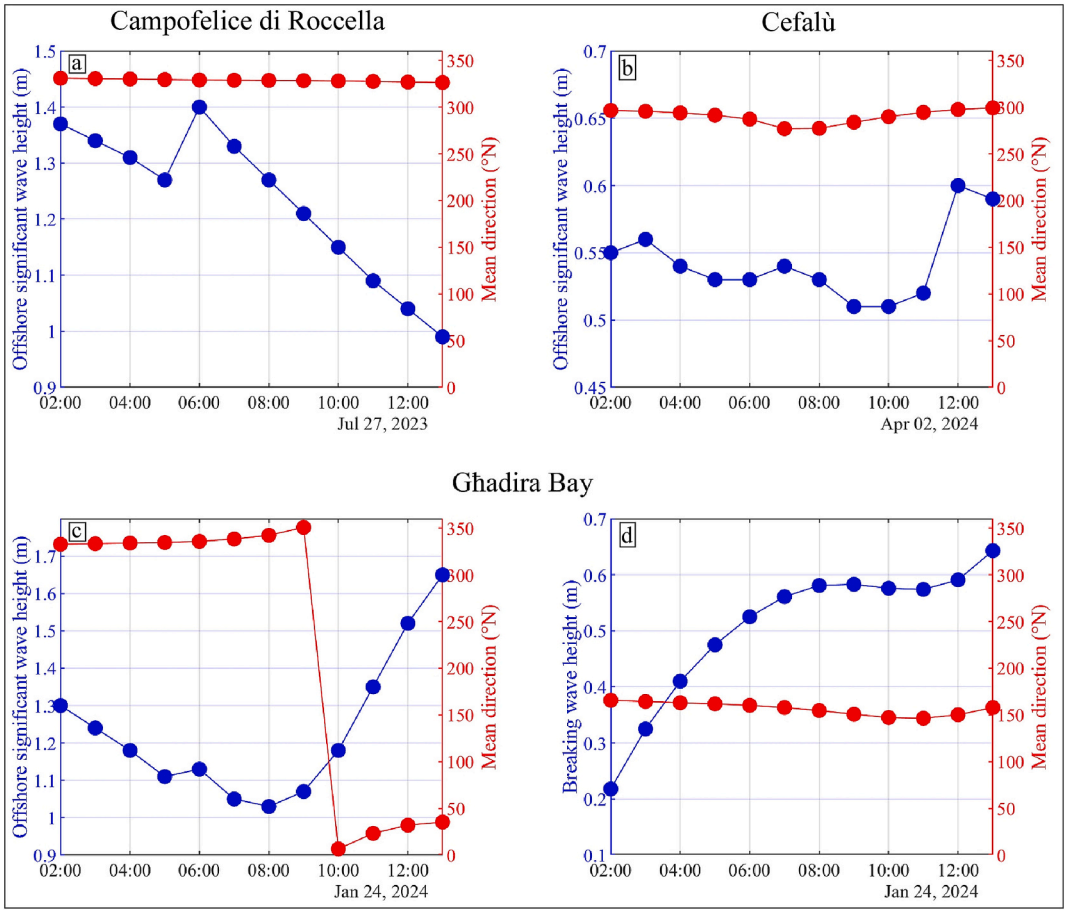

Fig. 4. Offshore wave height (blue line) and direction (red line) data downloaded from Copernicus Marine Service Information for a) Campofelice di Roccella site, b) Cefalù site and c) Għadira Bay site. In d) wave height (blue line) and direction (red line) data at the breaking point computed by the Rosario SWAN Wave Model from the i-waveNet project database for Għadira Bay site. (For interpretation of the references to colour in this figure legend, the reader is referred to the web version of this article.)

point, computed by the Rosario SWAN Wave Model (Fig. 4 d) from the i-waveNet project database (https://data.ocean.mt/oceanDataPortal/public/).

3.2. LST bulk formulas

Among the several available approaches, the LST rates for dry mass ($Q_{t,\ mass}$, kg/s) were calculated through three different bulk LST formulas (1), (2) and (3) proposed by CERC (1984), Kamphuis (1991) and Van Rijn (2014), respectively. The Eqs. (1) and (2) were selected because they are the most widely used in the literature, while the Eq. (3) formula was chosen because, in addition to being more recent, it was specifically calibrated for beaches with gravel-sized sediments.

$$Q_{t,mass} = 0.03k\rho g^{0.5}(H_b)^2(h_b)^{0.5}sin(2\theta_{br})\left[\frac{\rho_s}{(\rho_s-\rho)}\right] \quad (1)$$

$$Q_{t,mass} = 2.33(T_p)^{1.5}(tan\beta)^{0.75}(H_b)^2(D_{50})^{-0.25}[sin(2\theta_{br})]^{0.6}\left[\frac{\rho_s}{(\rho_s-\rho)}\right] \quad (2)$$

$$Q_{t,mass} = 0.00018\rho_s g^{0.5}(tan\beta)^{0.4}(H_b)^{3.1}(D_{50})^{-0.6}sin(2\theta_{br}) \quad (3)$$

where ρ is the mass density of seawater (1025 kg/m^3), g is the gravity acceleration (9.81 m/s^2), ρ_s is the mass density of the sediment (2650 kg/m^3), T_p (s) is the wave period at spectral peak, D50 (m) is the median grain size, H_b is the breaking wave height (m), h_b is the water depth at breaking point (m) and θ_{br} is the breaker angle. In formula (2), $tan\beta$ is the slope of the surf zone, whereas, in formula (3), it corresponds to the slope of the surf zone or the beach slope when the beach is sandy or gravelly, respectively. k is a dimensionless coefficient relating sand transport to longshore energy flux (0.2–1.6, Bodge and Kraus, 1991). We tested four k values: the minimum (0.2), the maximum (1.6), the most used in literature (0.39), and the average value (0.77).

The parameters H_b, h_b and θ_{br} were calculated by using Eqs. (4) and (5) proposed by Rattanapitikon and Shibayama (2006) and Eq. (6) by Larson et al. (2010), respectively. We chose Eqs. (4) and (5) because they provide good accuracy for the cases of $H_o/L_o \leq 0{,}1$ (Robertson et al., 2013).

$$H_b = \left(-0.57tan\beta^2 + 0.31tan\beta + 0.58\right)L_o\left(\frac{H_o}{L_o}\right)^{0.83} \quad (4)$$

$$h_b = \left(3.86tan\beta^2 - 1.98tan\beta + 0.88\right)H_o\left(\frac{H_o}{L_o}\right)^{-0.16} \quad (5)$$

$$\theta_{br} = arcsin\left(\sqrt{2\pi}\,sin\theta_o\sqrt{\frac{h_b}{L_o}}\right) \quad (6)$$

where θ_o is the angle between the offshore wave direction and the perpendicular to the coastline, H_o is offshore significant wave height, and L_o is the offshore wavelength that was estimated through the deep-water wave dispersion Eq. (7).

$$L_o = \frac{g}{2\pi}T_p{}^2 \quad (7)$$

3.3. Numerical model

We used XBeach 2DH numerical model to simulate nearshore and coastal hydrodynamic and morphodynamic processes (e.g. wave propagation, sediment transport, seabed morphological changes) at kilometer and storm time scales (Roelvink et al., 2009, 2010). The time-varying wave action balance solved in XBeach 2DH model in surfbeat mode is as follows:

$$\frac{\partial E}{\partial t}+\frac{\partial EC_{g,u}}{\partial s}+\frac{\partial EC_{g,v}}{\partial n}+\frac{\partial EC_{\vartheta}}{\partial \vartheta}=-Sink$$

where E is the wave energy or wave action, C_g is the group velocity, C_ϑ the refraction speed in theta-space and Sink refers to wave breaking and bottom friction effects.

Sediment accretion and erosion are modelled through the depth-averaged advection-diffusion equation (Galappatti and Vreugdenhil, 1985), calculating the difference between the actual depth-averaged sediment concentration and the equilibrium concentration (further details of theoretical background in (Roelvink et al., 2009, 2018). This approach allows us to estimate the sediment transport rate and to determine the seabed morphological changes at each time step.

We used the Surfbeat module in the 1.24.6057 Halloween XBeach 2DH model release to resolve the short-wave variations on the wave group scale and the associated long waves. Regarding the wave boundary conditions, we chose the time-varying JONSWAP spectrum with a duration of 1 h for a single spectrum and 12 h for the whole simulation. Local wind and tidal set-up were not considered in the model set-up.

The sediment transport rate was calculated using the Van Rijn (1993). The initial water level (z0) was set to zero, the morphological acceleration factor (morfac) was set to 1 and the simulation time was adapted to the morfac (morfacopt = 1). The grain size of the seabed is set using D50 and D90 sediment fractions derived from grain size analysis of seabed samples (see Section 3.1.3).

The computational domain extends from the emerged area up to 20 m of depth (Fig. 5 a, b and c), corresponding to the input wave parameters' depth provided by the Copernicus database (see Section 3.1.4). To generate the model grid and merge bathymetric and topographic datasets, we used the Deltares Open Earth Toolbox in MATLAB (https://oss.deltares.nl/web/xbeach/tools). We set a grid with variable-size cells in x direction. The cell size was calibrated to find a good

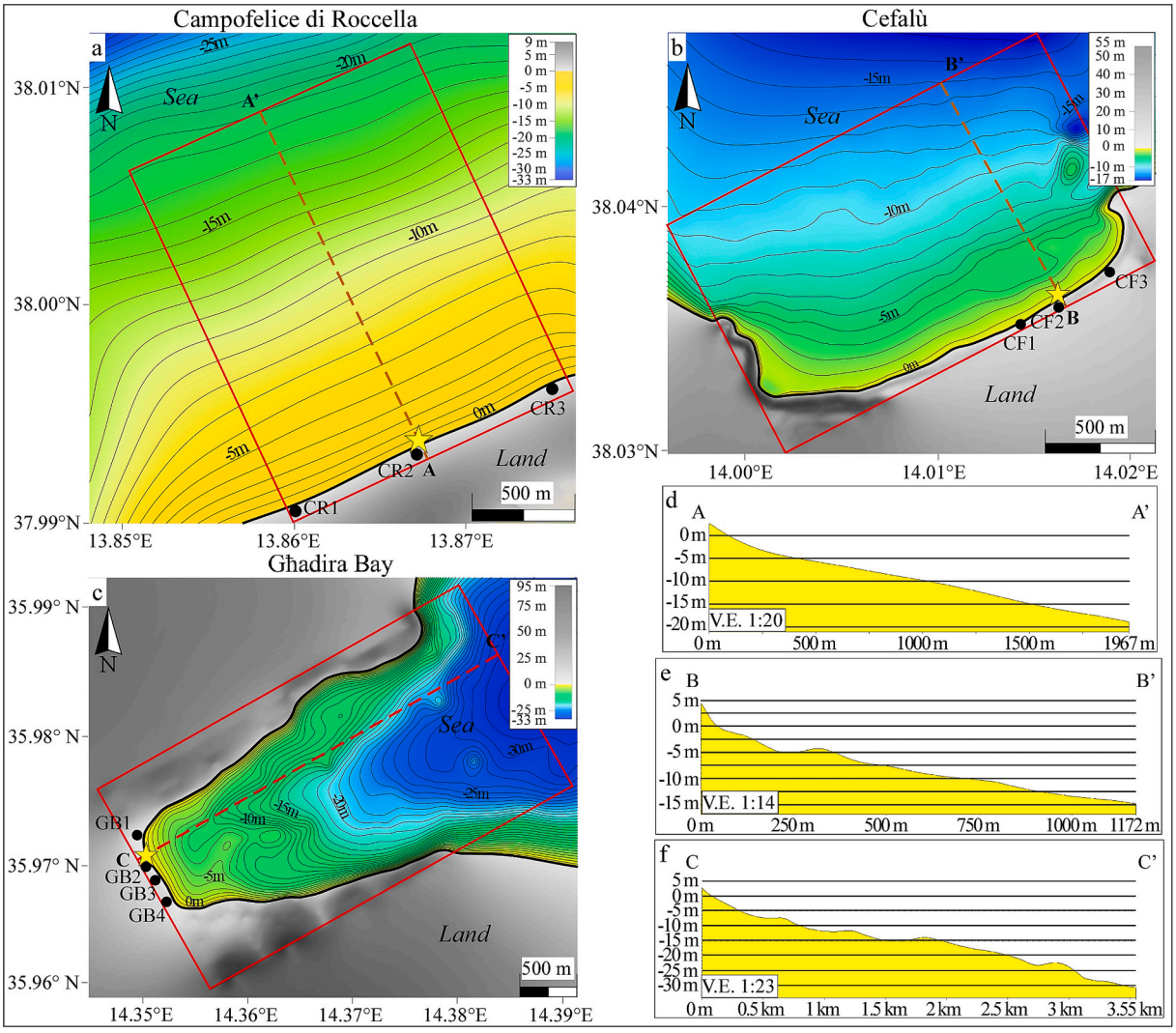

Fig. 5. Topobathymetric maps of a) Campofelice di Roccella, b) Cefalù and c) Għadira Bay. The stars indicate the position of LST rate measurements using the streamer trap and surf zone seabed sediment sampling. The black dots indicate the position of the collected beach sediment samples. The red rectangles indicate the limits of XBeach 2DH models' computational domain. The dashed orange lines AA' (a and d), BB' (b and e) and CC' (c and f) show the bathymetric profiles crossing the streamer trap location (transects CTL, see Section 4.1). (For interpretation of the references to colour in this figure legend, the reader is referred to the web version of this article.)

compromise between number of cells and computational time. The grid consists of cells with a maximum size of 10 m for CR and GB sites and 5 m for CF site in sectors with water depths greater than closure depth (Hallermeier, 1981). For depths below the wave/seabed interaction depth, the cell size decreases landward from the maximum value (10 m for CR and GB sites and 5 m for CF site) to the minimum of 0.5 m. The XBeach 2DH model parameter set of computational domains (e.g. cell corners, cell dimensions, directional limits, directional resolution) is reported in Table S1.

To achieve the best fit between the model results and field data, we conducted the modelling by considering the specific characteristics of the study areas, such as wave data, grain size, and morphology. To do this, we calibrated the sediment transport parameters (e.g. facua, bdslpeffmag, facsl, bdslpeffini, reposeangle, form, lws, turb; Table 1) and morphology parameters (e.g. wetslp, morfac, morfacopt; Table 1). We chose these two parameters sets because they are considered the most influent on the LST by several authors (Bugajny et al., 2013; Elsayed and Oumeraci, 2017; Hwang et al., 2024; Satheeshkumar and Balaji, 2021). Moreover, we calibrated the parameter "alfaD50" to improve the sensitivity of the LST formulas to grain size, as indicated in the release note of the software XBeach 2DH model v. 1.24.6057 (Table 1).

The calibration process involved first varying each parameter individually to assess its impact on the model's predictions and identify optimal values. We then combined these parameters in various configurations to improve the model's accuracy. Due to the different characteristics of the study areas, we chose different calibrations for GB and CR sites and validated the parametrization of GB site in the CF site. The list of calibrated parameters and the used values is shown in Table 1. The vegetation module of XBeach 2DH model was used to model the dissipation mechanism of short and long waves caused by seabed vegetation in the GB site. We schematized the vegetation in vertical elements and considered its characteristics (e.g. height from the seabed, stem diameter, density) from literature data (Borg et al., 2005).

To calculate the LST rates, we averaged the values obtained at 11:00 am, 11:30 am, 12:00 am and 12:30 pm in the closest cell to the field measurement point for each site. The time interval 11:00–12:30 was chosen because it corresponds with the field measurement timing. The associated error bar is calculated as the standard deviation between the considered values.

4. Results

4.1. Morphology of the study areas

The CR site is a 3.1 km^2 wide-open system. The emerged beach is about 1.5 km long in the ENE-WSW direction and 40 m wide from the coastline landward. The maximum elevation value is 5 m and decreases seaward with an average slope of 1.4°. The slope is 1.7° along the transect that crosses the streamer trap location (transect CTL, Fig. 5 a and d). The submerged sector extends up to 1.8 km from the coastline and reaches 20 m of water depth (Fig. 5 a). Based on the wave heights considered for this study, the surf zone reaches depths of about 1.8 m and elongates seaward for 77 m from the coastline with a slope of 1.35°, measured along the transect CTL (Fig. 5 d). From the surf zone to offshore, the seabed gradually deepens with a constant slope, as suggested by the equidistant contours (Fig. 5 a).

The CF site is an embayed system that covers an area of 2.2 km^2. The site is bounded on its northern and southern sides by headlands, which extend 560 m and 290 m seaward and elevate up to 52 m and 3.6 m, respectively. The emerged beach is about 1.7 km long in the NE-SW direction and up to 2.5 m high along its landward boundary. From there, the beach extends 25 m to the coastline with an average slope of about 4°. Whereas the beach slope reaches 5.1° along the transect CTL (Fig. 5 b and e). The submerged sector is up to 1.1 km long from the coastline and is characterized by depths of up to 17 m. The surf zone elongates 50 m seaward with a slope of 1.44°, measured along the transect CTL (Fig. 5 b and e), and reaches 1.3 m of depth. From the surf zone to offshore, the slope decreases gradually, as indicated by the increase of the mutual distance of the contour lines, locally interrupted by slope breaks (Fig. 5 b).

The GB site is an embayed system of 7 km^2 that consists of an emerged beach trending in the NNW-SSE direction and limited by headlands on both sides. The northern and southern structural highs elongate for 3 km and 2.4 km seaward, respectively, and show a maximum elevation of 60 m and 89 m. The emerged beach is about 900 m long and up to 2 m high (Fig. 5 c and f). It shows a width of 40 m from the coastline landward and an inclination of 1.3° along the transect CTL. The submerged sector extends about 3.5 km from the coastline and up to 30 m in depth (Fig. 5 c). The surf zone is 28 m long and reaches a maximum water depth of 1 m with a slope of 1.36°, measured along the transect CTL (Fig. 5 c and f). From the surf zone to offshore, the seabed is

Table 1
Calibrated parameters and used values for Għadira Bay (GB), Cefalù (CF) and Campofelice di Roccella (CR) sites.

Parameter and Description	Default value	Range value	Tested value	Used value for GB and CF sites	Used value for CR site
facua - Calibration factor time averaged flows due to wave skewness and asymmetry	0.175	0.0–1.0	0.02, 0.1, 0.35, 0.175	0.35	0.35
alfaD50 - Calibration coefficient for grain size term	0.4	0–1	0 0.25, 0.4, 0.75, 1	0.25	0.4
bdslpeffmag - Modify the magnitude of the sediment transport based on the bed slope	roelvink_total	none, roelvink_total, roelvink_bed, soulsby_total, soulsby_bed	None, roelvink_bed, soulsby_bed, soulsby_total, roelvink_total	soulsby_bed	soulsby_bed
facsl - Factor bedslope effect	1.6	0–1.6	0, 0.15, 0.8, 1.6	1.6	1.6
bdslpeffini - Modify the critical shields parameter based on the bed slope	none	none, total, bed	total, bed, none	total	total
reposeangle - Angle of internal friction	30	0–45	30, 35, 40	30	35
form - Equilibrium sediment concentration formulation	vanthiel_vanrijn	soulsby_vanrijn, vanthiel_vanrij, vanrijn1993	soulsby_vanrijn, vanthiel_vanrij, vanrijn1993	Vanrijn1993	Vanrijn1993
lws - Switch to enable long wave stirring	1	0–1	0, 1	0	0
turb - Switch to include short wave turbulence	wave_averaged	none, wave_averaged, bore_averaged	none, wave_averaged, bore_averaged	none	none
wetslp - Critical avalanching slope under water	0.15	0.1–1	0.15, 0.1, 0.5, 1	0.15	0.15
morfac - Morphological acceleration factor	1	0.0–1000.0	0, 1	1	1
morfacopt - Switch to adjusting output times for morfac	1	0–1	0, 1	1	1

characterized by a decreasing slope suggested by the seaward increase of the mutual distance of the contour lines. In the western sector, between 0.5 km to 3 km from the coastline, the seabed shows an irregular morphology with several slope breaks (Fig. 5 c and f).

4.2. Granulometric analysis

Granulometric analysis was performed on sediment samples collected from the surf zone seabed and from the beach face (Fig. 5 a, b and c for location).

Three beach samples, collected in the CR site (Fig. 5 a for location), are defined by D50 values ranging between 0.36 mm and 1.26 mm, with an average value of 0.72 mm (Fig. 6 a). Whereas the D90 values are from 0.75 mm to 6.37 mm, with an average of 3 mm. The seabed sample (Fig. 5 a for location) has a D50 value of 6.33 mm and a D90 value of 239.97 mm (Fig. 6a).

Three beach and seabed samples were collected at the CF site (Fig. 5 b for location). Beach samples are characterized by D50 values ranging from 0.19 mm to 0.56 mm, with an average value of 0.42 mm (Fig. 6 b). D90 values vary from 0.34 mm to 0.93 mm, with an average value of 0.71 mm. The seabed sample yields a D50 value of 0.69 mm and a D90 value of 7.96 mm (Fig. 6 b).

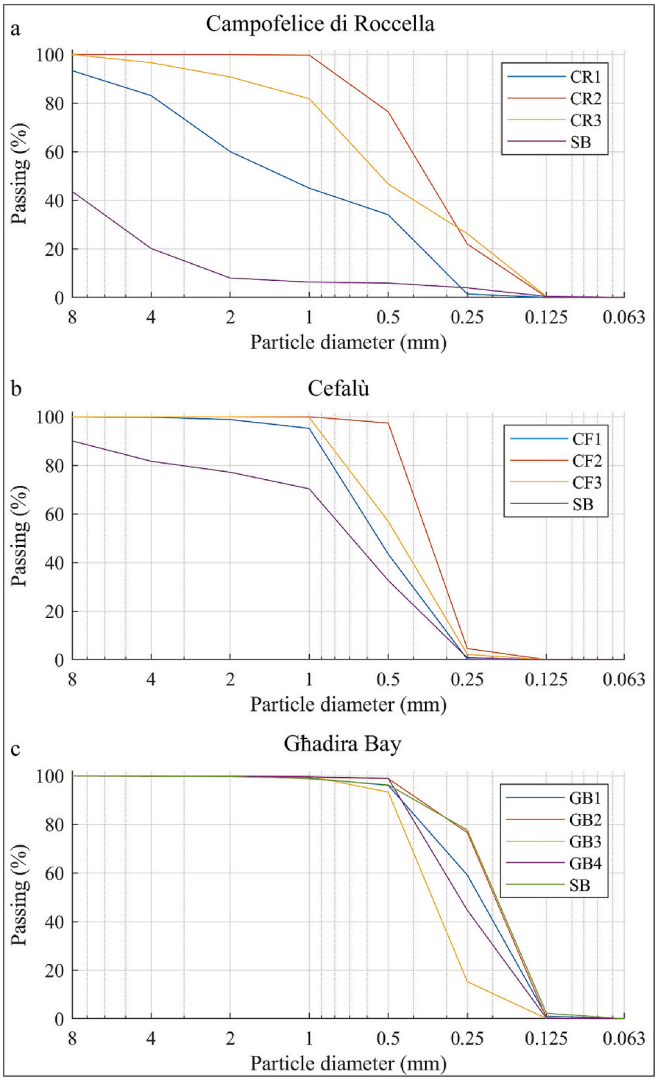

Fig. 6. Grain size curves of seabed (SB) and beach samples collected in a) Campofelice di Roccella site (CR1, CR2, CR3), b) Cefalù site (CF1, CF2, CF3) and c) Għadira Bay site (GB1, GB2, GB3, GB4). See Fig. 5 for sample locations.

Four beach and seabed samples were taken at the GB site (Fig. 5 c for location). Regarding the beach samples, the average value of D50 is 0.26 mm, with a maximum value of 0.34 mm and a minimum of 0.20 mm (Fig. 6 c). Whereas the D90 averaged 0.44 mm, ranging from 0.38 mm to 0.49 mm. The seabed sample is defined by values of 0.19 mm and 0.40 mm for D50 and D90, respectively (Fig. 6 c).

4.3. Marine vegetation in the Għadira Bay site

The distribution map of seabed vegetation in the GB site (Fig. 7) was obtained by UAV images investigating an area of 1.48 km^2 (see Fig. 7 for the seaward limit of the study area). The map shows patchy beds of vegetation that cover an area of 0.8 km^2. On the northern and southern sides of the GB site, marine vegetation extends from the coastline to a depth of 10 m. In the western sector, it is recognised as starting at least 150 m from the coastline seaward and reaching a maximum depth of 15 m in the central sector.

According to Borg et al. (2005), the vegetation type is *P. oceanica*, characterized by an average leaf width and length of 0.8 cm and 45 cm, respectively, and a shoot density of 27/0.05 m^2.

4.4. Wave parameters

We used offshore wave parameters (Table S2, Fig. 4 a, b and c), derived from the Copernicus database (see Section 3.1.4), to estimate the LST rates by XBeach 2DH modelling and bulk formulas. To apply the bulk formulas, we calculated I) L_o and θ_o (Table 2) using the equations described in Section 3.2; II) the wave-breaking parameters (H_b, θ_{br}, h_b in Table 2) using the mean value of the offshore wave parameters (H_o, D_{ir}, T_p in Table 2) recorded in the time interval that is the closest to the time of the field LST measurements; III) tanβ, where β is the slope of the surf zone or the beach slope depending on the used formula (see Section 3.2). The parameter values, used in the bulk formulas, are summarized in Table 2.

For the GB site, we also used wave parameters (H_b, D_{ir} and T_p) from Rosario SWAN wave model (Fig. 4 d) and corresponding with mean values of 0.58 m, 148°N and 9.23 s, respectively. We considered these data to estimate θ_{br} and h_b through Eqs. (6) and (5) described in Section 3.2. The obtained values are 88° for the θ_{br} and 1.16 m for h_b.

4.5. LST rate results

The LST rates were determined using three methods: field measurements by the streamer trap, bulk formulas, and XBeach 2DH model.

The average values of LST rate, derived from two field measurements for each site (Table 3), are $3.69{\cdot}10^{-03} \pm 9.6{\cdot}10^{-04}$ kg/s in the CR site, $3.19{\cdot}10^{-03} \pm 4.0{\cdot}10^{-04}$ kg/s in the CF site and $1.04 \cdot 10^{-03} \pm 2.6 \cdot 10^{-04}$ kg/s in the GB site.

The LST rate values, obtained by bulk formulas, were schematised in Table 4. We specify that the CERC formula (1984) result reported in Table 4 was obtained considering the k value of 0.2. We tested the other three k values (see Section 3.2 and Table 5) and chose the formula result derived from the minimum k value of 0.2 because it is the closest to the measured LST rate.

XBeach 2DH calibrated model results are shown in Fig. 8. The curves represent the LST rate values along the longshore transect intersecting the field measurement points. The modelled LST rates are calculated as the average of the values obtained at 11:00 am, 11:30 am, 12:00 pm and 12:30 pm in the cell of the model closest to the field measurement point for each site (black circles in Fig. 8). The average LST rates are $2.93{\cdot}10^{-03} \pm 3.1{\cdot}10^{-04}$ kg/s for the CR site and $5.66{\cdot}10^{-03} \pm 4.7{\cdot}10^{-03}$ kg/s for the CF site. At the GB site, we computed the LST rate both considering the presence of *P. oceanica* on the seabed (Fig. 8 d) and without it (Fig. 8 c). The average LST rates are $1.95{\cdot}10^{-03} \pm 1.6{\cdot}10^{-03}$ kg/s and 2.9 ± 0.5 kg/s, respectively with/without the marine vegetation.

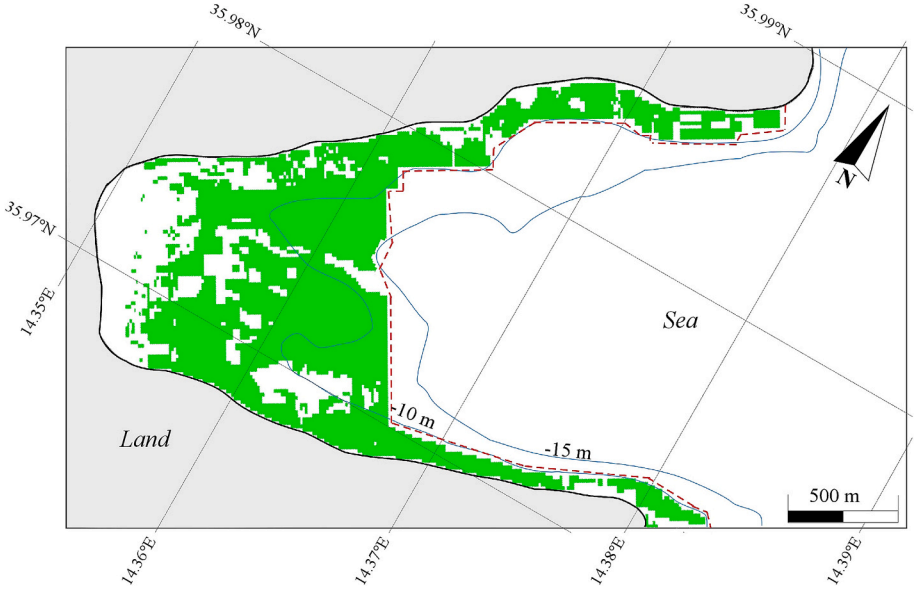

Fig. 7. Map of Posidonia oceanica distribution on the Għadira Bay seabed. The green cells indicate the presence of marine vegetation. The solid black line represents the coastline, the dashed red line represents the seaward limit of the investigated area. The blue lines are the isobaths of 10 m and 15 m. (For interpretation of the references to colour in this figure legend, the reader is referred to the web version of this article.)

Table 2
Parameter values used in the bulk formulas.

Parameters for bulk formulas									
Site	H_0 (m)	D_{ir} (°N)	T_p (s)	L_o (m)	θ_o	H_b (m)	θ_{br} (degree)	h_b (m)	tanβ
Għadira Bay	1.44	27.64	8.39	109.90	32.00	1.76	11.34	2.41	0.02
Cefalù	0.72	296.96	8.39	109.90	28.04	0.99	7.47	1.34	0.03
Campofelice di Roccella	1.04	326.81	7.63	90.82	8.19	1.31	2.86	1.78	0.02 (surf zone) 0.03 (beach)

Table 3
LST values derived from field measurements by streamer trap. Values 1 and 2 were obtained by measurements in the time interval, respectively, between 11:30–11:40 am and 12:10 and 12:20 pm on 27th July 2023 at the Campofelice di Roccella site, on 24th January 2024 at the Għadira Bay site, and 2nd April 2024 at the Cefalù site.

Field measured LST rate (kg/s)		
Site	Value 1	Value 2
Għadira Bay	$9.08 \cdot 10^{-04}$	$1.16 \cdot 10^{-03}$
Campofelice di Roccella	$4.17 \cdot 10^{-03}$	$3.21 \cdot 10^{-03}$
Cefalù	$2.99 \cdot 10^{-03}$	$3.40 \cdot 10^{-03}$

Table 4
LST rate computed by bulk formulas in each study area. In the Għadira Bay site, bulk formulas were tested using H_b derived from empirical formula (H_bEF) and Rosario database (H_bRD).

LST rate (kg/s) computed by bulk formulas				
Formula	Għadira Bay		Campofelice di Roccella	Cefalù
	(H_bEF)	(H_bRD)		
CERC (1984)	60.84	0.71	7.43	9.65
Kamphuis (1991)	80.25	3.28	7.31	15.77
Van Rijn (2014)	123.98	0.61	1.74	6.84

5. Discussions

As previously mentioned, to identify the most accurate method for estimating LST in three different coastal settings on Malta Island and northern Sicily, we computed the LST rate using three different bulk formulas and XBeach 2DH model. The predictions from the formulas and the model were then compared with the field-measured LST rate. This section is devoted to comparing and discussing the results obtained by considered approaches, in order to identify the potential and limitations of each one. The comparison between the LST rate values derived from empirical formulas and numerical models, as well as the overestimation and underestimation factors of LST rate values to respect the field data, are shown in Figs. 9 and 10, respectively.

Table 5
LST rate computed using CERC formula (1984), varying k value in each study areas. In Għadira Bay site, bulk formulas were tested using H_b derived from empirical formula (H_bEF) and Rosario database (H_bRD).

LST rate (kg/s) derived from CERC formula (1984)				
Site k	0.20	0.39	0.77	1.60
Għadira Bay (H_bEF)	60.84	118.63	234.22	486.69
Għadira Bay (H_bRD)	0.71	1.38	2.73	5.67
Campofelice di Roccella	7.43	14.49	28.62	59.46
Cefalù	9.65	18.82	37.15	77.19

5.1. Comparison between bulk formulas' results and observations

LST rate estimations based on the CERC (1984) and Kamphuis (1991) formulas show respectively an overestimation factor of 1857 and 1827 in the CR site, 4825 and 7885 in the CF site, 710 and 3280 in the GB site (considering formulas with H_b value from Rosario database; Fig. 10). Despite the results of Van Rijn formula (2014) representing the lowest values for all study areas (Fig. 9), they have an overestimation factor of

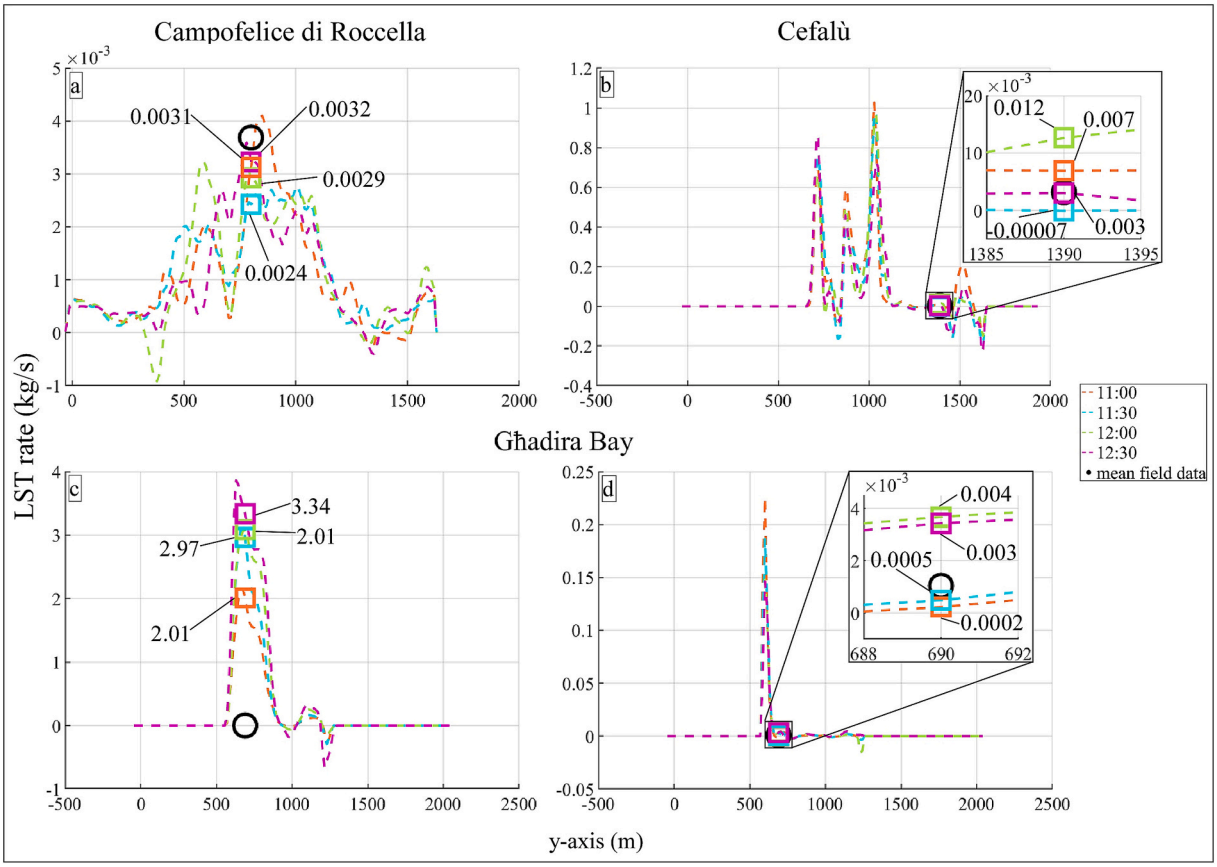

Fig. 8. Graphs of LST rates derived from XBeach 2DH model at a) Campofelice di Roccella, b) Cefalù, c) and d) Għadira Bay. The curves show the LST rate values along the longshore transect that intersects the field measurement points. The average field measurements are indicated by black circles. The modelled LST rates are calculated for the time intervals closest to the field measurement times: 11:00 am (orange dashed line), 11:30 am (blue dashed line), 12:00 pm (green dashed line) and 12:30 pm (purple dashed line). Graphs (c) and (d) display the LST rates at Għadira Bay calculated without and with consideration of the presence of P. oceanica on the seabed, respectively. Insets provide a zoomed view of the results. (For interpretation of the references to colour in this figure legend, the reader is referred to the web version of this article.)

435 in the CR site, 3420 in the CF site, 610 in the GB site (considering the formula with H_b value obtained from Rosario database; Fig. 10).

The misfit between the value of LST rate, predicted by bulk formulas, and the field measurements were widely documented in previous studies (Bodge and Kraus, 1991; Eversole and Fletcher, 2003; Mil-Homens et al., 2013; Pereira Quadrado and Goulart, 2020; Salem Cherif et al., 2019; Sanil Kumar et al., 2003; Shanas and Sanil Kumar, 2014; Wang et al., 1998; Williams et al., 2008). These researchers focused on studying the parameters that influence the LST rate value to improve the accuracy of the bulk formulas. According to Van Rijn (2003) and Pereira Quadrado and Goulart (2020), the accuracy of the formulas' results depends on the accuracy of the wave parameters, which is related to the method used to calculate them. We tested how the accuracy of the wave parameters influences the LST rate in the GB site. To do this, we used H_b values obtained from the empirical formula Eq. (4) (see Section 3.2) and Rosario database. The latter is computed using SWAN wave model that considers the processes of propagation, generation, dissipation and nonlinear wave-wave interactions (Booij et al., 1996). For this reason, the SWAN wave model is considered more accurate than the empirical formula derived from laboratory data (Rattanapitikon and Shibayama, 2006). Our findings highlight that the bulk formula results are up to 200 times lower when we use H_b values derived from the Rosario database (formulas with H_bRD in Fig. 9 c) than H_b values derived from the empirical formula (formulas with H_bEF Fig. 9 c). Although using a more accurate wave parameter allowed us to reduce the gap between the field measurement and the bulk formulae results, these values are still overestimated by a factor of up to 3280 compared to the measured LST rate value (Fig. 10). However, a limitation of our study is the availability of the SWAN model data only for the GB site. We could not apply this more accurate approach across all three sites, which may have further refined our understanding of the discrepancies observed in LST rate predictions.

The accuracy of the formulas also results from the calibration of key parameters that influence the LST rate (Rosati, 2005; Wang and Kraus, 1999), such as the wave height and the grain size. Wang et al. (1998) recommended using the CERC formula (1984) in storm conditions where H_s exceed 4 m. The study areas of this research are characterized by low wave conditions with H_s values of about 1 m. Thus, the LST rate values derived from the CERC formula (1984) are overestimated probably because the wave conditions of our sites are different from those recommended by Wang et al. (1998) for the best performance of the CERC formula (1984). Moreover, since it is impossible to acquire measurements with wave heights exceeding 1 m due to the manual installation of the trap and the possibility of its overturning, it is impractical to compare our results under the optimal conditions suggested for the CERC formula (1984). In other areas under low wave conditions, Shanas and Sanil Kumar (2014) obtained overestimated LST rates of factor 1.7 using the CERC formula (1984), whereas Van Rijn (2014) obtained overestimated LST rates of factor 5 and 3 using the CERC (1984) and Kamphuis (1991) formulas, respectively.

Regarding the grain size, a different weight was assigned to it by bulk formulas through an exponential function. Kamphuis (1991) empirically determined the exponent of D50 and found that the LST rate is inversely proportional to $D50^{0.25}$. This result indicates that sediment transport depends only slightly on grain size. Conversely, other studies highlight a

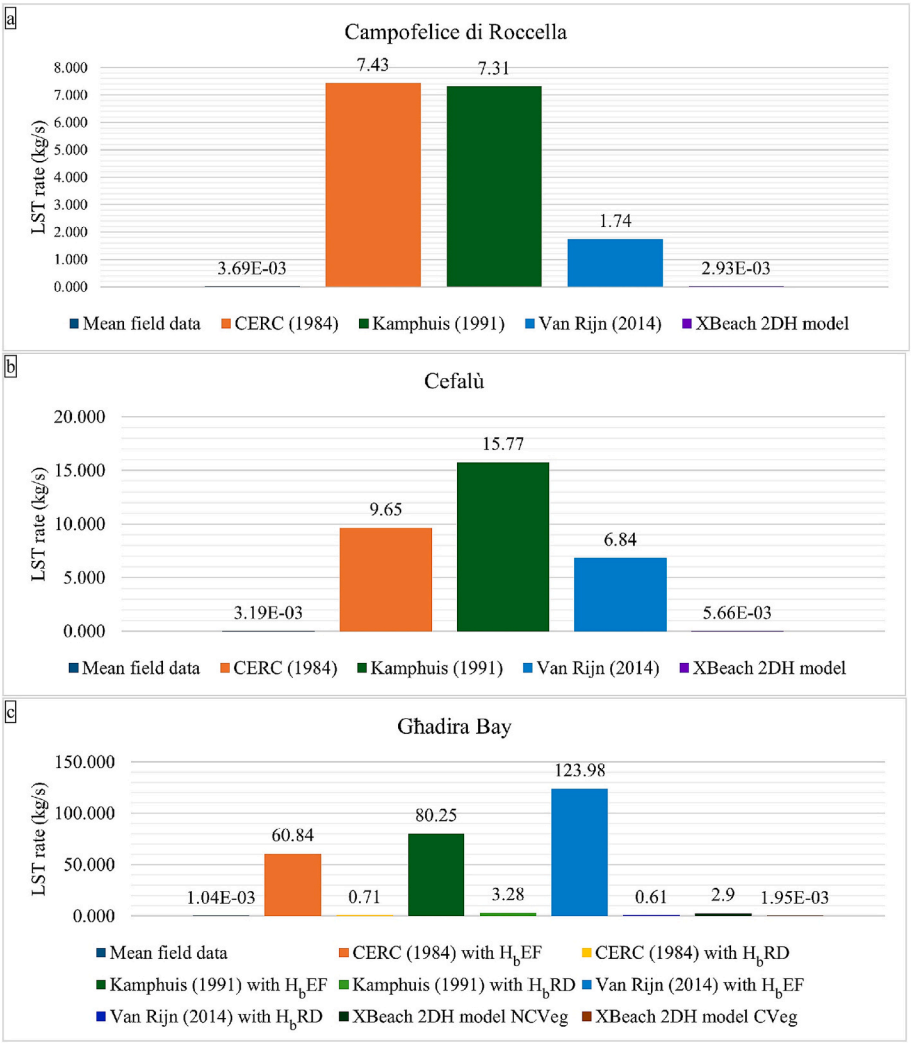

Fig. 9. LST rate values measured by streamer trap and computed by bulk formulas and XBeach 2DH model at a) Campofelice di Roccella, b) Cefalù and c) Għadira Bay sites. In the latter site, the performance of bulk formula was tested using H_b derived from empirical formula (H_bEF) and Rosario database (H_bRD), while the performance of the XBeach 2DH model was evaluated not considering the presence of marine vegetation (NCVeg) and considering it (CVeg).

stronger dependence of the LST rate on the grain size (Mil-Homens et al., 2013; Tomasicchio et al., 2013; Van Rijn, 2014). Among these, Van Rijn (2014) assigned to D50 an exponent through numerical models and found that LST rate is inversely proportional to $D50^{0.6}$. Our results show that LST rates predicted by the Van Rijn formula (2014) align more closely with the measured data compared to those from the Kamphuis formula (1991) across all study areas (Fig. 9). This finding confirms the strong dependence of the LST rate on the grain size. Although the Van Rijn formula (2014) is more accurate than the Kamphuis formula (1991), the results overestimate those measured in the field. The discrepancy is probably due to the wave conditions ($\theta_o = 30°$, $H_s = 3$ m, $T_p = 8$ s) used by Van Rijn (2014) to calibrate the D50, which are not representative of the average conditions of our study areas.

The D50 value is not considered a parameter in the CERC formula (1984). However, the formula includes the parameter k, which is linked to several factors, such as the grain size and breaker type (Rosati et al., 2002; Wang and Kraus, 1999). Several authors tried to calibrate k to improve the LST rate estimated by the CERC formula (Bodge and Kraus, 1991; del Valle et al., 1993; Eversole and Fletcher, 2003; Schoonees and Theron, 1993; Van Wellen et al., 2000). In our study, we tested four *k* values in the range proposed by Bodge and Kraus (1991): the minimum (0.2), the maximum (1.6), the most used in literature (0.39), and the average value (0.77). The obtained LST rate values are overestimated in our study areas (see Table 5), both with fine sand (GB site), coarse sand (CF site) and gravel (CR site). Despite the use of different k values, previous studies highlighted that CERC formula (1984) results generally overpredict the LST rate up to 3000 % (Bayram et al., 2007; Bodge and Kraus, 1991; Eversole and Fletcher, 2003; Pereira Quadrado and Goulart, 2020; Salem Cherif et al., 2019; Shanas and Sanil Kumar, 2014; Wang et al., 1998, 2002). Thus, it would be appropriate to improve the calibration of k and not use a single value of k for all longshore transport conditions.

Another factor that controls the LST rate is the presence of marine vegetation on the seabed. The vegetation limits the erosion of sediments, dissipating the energy of the currents on the bottom and reducing the shear stress at the sediment-water interface (Le Hir et al., 2007; Widdows and Brinsley, 2002). The two actions cause, in turn, a decrease in the LST rate. This condition occurs in the GB site, where the seabed is covered by *P. oceanica*. Therefore, the overestimation of the LST rates is partly due to neglecting marine vegetation as a parameter of the bulk formulas.

5.2. Comparison between XBeach 2DH model results and observations

XBeach 2DH model results indicate a good agreement between modelled values and field measurements (Figs. 8 and 9). The average

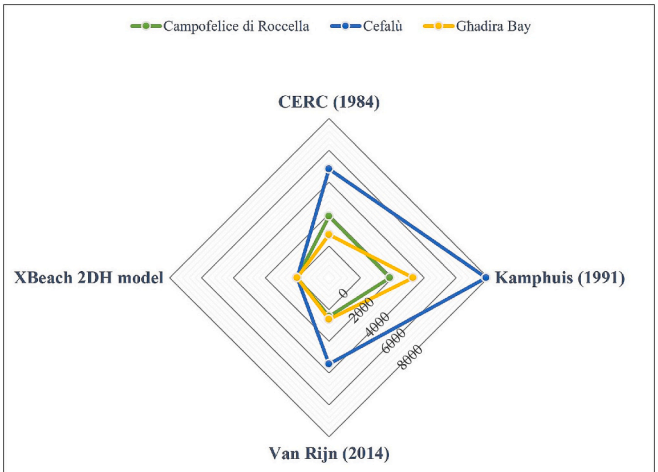

SITE	CERC (1984)	Kamphuis (1991)	Van Rijn (2014)	XBeach 2DH model
Campofelice di Roccella	1857	1827	435	-0.5
Cefalù	4825	7885	3420	1.8
Għadira Bay	710	3280	610	1.9

Fig. 10. Radar chart showing the overestimation and underestimation factors of LST rates derived from bulk formulas and numerical model. Values are referred to the field measurement. Factor values correspond to the vertexes of the lines for each site. The green, blue and yellow lines represent Campofelice di Roccella, Cefalù, and Għadira Bay, respectively. The table below summarizes the overestimation and underestimation factors of the LST values for each site. For the Għadira Bay site, the overestimation factor refers to bulk formulas that use H_b values derived from Rosario database. (For interpretation of the references to colour in this figure legend, the reader is referred to the web version of this article.)

modelled and measured LST rates are, respectively, 0.003 kg/s and 0.004 kg/s in the CR site, 0.006 kg/s and 0.003 kg/s in the CF site, 0.002 kg/s and 0.001 kg/s in the GB site.

Previous studies suggest calibrating the model based on specific characteristics (e.g. wave data, grain size, morphology) of the study area and fine-tuning the model result until the output fits with field data (Bergillos et al., 2017; Elsayed and Oumeraci, 2017; Garzon et al., 2022; Hwang et al., 2024; Jin et al., 2021; McCall et al., 2010; Satheeshkumar and Balaji, 2021; Simmons et al., 2019; Simmons and Splinter, 2022). We calibrated the model based on parameters (see Section 3.3) that are considered the most influential on the LST rate (Bugajny et al., 2013; Elsayed and Oumeraci, 2017; Hwang et al., 2024; Satheeshkumar and Balaji, 2021; XBeach User Manual v. 1.24.6057).

The model results of the GB site are in good agreement with those obtained from field observations (Figs. 8 d and 9 c), showing an overestimate of factor 1.9 (Fig. 10). The good performance of the model in the GB site is due to the calibration and also to possibility to include the presence of *P. oceanica* on the seabed into the modelling. We tested the model both with and without the "vegetation module" to verify the influence of marine vegetation on the LST rate. Our results show that LST rate significantly reduces from 2.9 kg/s to 0.002 kg/s when the model includes marine vegetation, fitting the field measurement of LST rate (0.001 kg/s). This finding further confirms that vegetation plays a key role in controlling the LST rate, consistent with the studies by Widdows and Brinsley (2002) and Le Hir et al. (2007).

The calibration values applied to the GB site were successfully validated in the CF site, where the model result overestimated by a factor of 1.8 the field measurement (Fig. 10). The calibration showed a good performance because both the GB and CF sites have similar characteristics of morphology (embayed system) and grain size (fine/coarse sand). Conversely, the parametrization used for the GB site provides a bad result in the CR site, overestimating the field measurement by a factor of 8. This result is probably due to the characteristics of the CR site, which is an open system with a gravelly beach. Therefore, different values of the parameters were chosen for the calibration of the CR site (see Table 1). The modelling provides a good result, underestimating the field value by a factor of 0.5 (Fig. 10).

Despite the D50 of the surf zone at the CR site being coarser than the recommended range for the XBeach 2DH model, the model performs well. Moreover, the modelling value for the CR site (0.003 kg/s) shows a better fitting with the field measurement (0.004 kg/s) compared to that calculated (1.74 kg/s) by the Van Rijn formula (2014), which is commonly used in literature for gravelly beaches. Figs. 9 a and 10 illustrate that the XBeach model calibrated for gravelly beaches provides a more accurate prediction of LST than the Van Rijn formula in the CR site.

Additionally, it must be pointed out that other sources of discrepancy between modelling values and observations may also be partly found in the error of the field measurement method to capture the sediment. In fact, the trap may oversample due to the stirring of seabed sediments caused by its placement, and undersample because the trap structure partly obstructs the sediment transport along the seabed. Undersampling can also result from the space between the seabed and the first bag, as well as the gaps between the trap's bags, which can prevent the capture of all sediment particles moving along the seabed and suspended in the water column. Future studies will focus on enhancing the quality of measured LST by improving sediment capture methods and conducting measurements under variable wave conditions to better understand and address these sources of error.

6. Conclusions

This research assesses the predictive capacity of three of the most commonly used bulk formulas (CERC, 1984; Kamphuis, 1991; Van Rijn, 2014) and the XBeach 2DH model (Roelvink et al., 2009) for estimating the LST rate in three different coastal settings located in Malta Island (Għadira Bay) and northern Sicily (Cefalù and Campofelice di Roccella sites). For each site, we have analysed the wave parameters (H_o, T_p, D_{ir}, H_b, $T_{p,br}$, $D_{ir,br}$), the grain size of the beach and seabed, the coastal type (open or embayed system), the seabed morphology and the presence of marine vegetation. Moreover, we have estimated the field LST rates and compared the field measurement to the results of applying both formulas and model.

Our finding highlights that the XBeach 2DH model is more accurate than bulk formulas in all the studied sites. Although previous studies have attempted to improve the bulk formulas by calibrating the parameters that control the LST rate, there is still a misfit between predictions and observations. Our results indicate overestimation factors of CERC formula (1984) ranging from 710 to 4825, Kamphuis formula (1991) ranging from 1827 to 7885, and Van Rijn formula (2014) ranging from 435 to 3420 (Fig. 10). This deviation may be due to several reasons, among these: a) not considering the 3D-morphological features of the emerged area (open and embayed system) and the seabed; b) the use of coefficients (k in the CERC formula (1984), the exponents of D50 in the Kamphuis formula (1991) and Van Rijn formula (2014)) that were calibrated based on boundary conditions (e.g. wave height, period, theta, grain size, breaker type) that are not representative of different world regions; c) the neglect of the vegetation on the seabed.

Conversely, the XBeach 2DH model results fit the field measurements, showing an overestimate of a factor of 1.9 in the GB site and 1.8 in the CF site and an underestimate of a factor of 0.5 in the CR site. The enhanced accuracy of the numerical model is due to its ability to represent the interactions between hydrodynamics and the LST processes by integrating site-specific factors (e.g. wave parameters, grain size and seabed/emerged morphology, presence of marine vegetation) that influence the LST rate.

To obtain the best performance of the XBeach 2DH model, we recommend using the closest wave data to the coastline and extending

the model grid seaward until the point corresponding with the wave data location. Moreover, we suggest calibrating the sediment transport parameters (e.g. facua, bdslpeffmag, facsl, bdslpeffini, reposeangle, form, lws, turb) and morphology parameters (e.g. wetslp, morfac, morfacopt) that are considered the most influent on the LST by several authors (Bugajny et al., 2013; Elsayed and Oumeraci, 2017; Hwang et al., 2024; Satheeshkumar and Balaji, 2021) and add the parameter "alfaD50" to the calibration set as indicated in the release note of the software XBeach 2DH v. 1.24.6057.

The research findings indicate that the parameter values used for the model calibration in this study can be applied successfully in embayed systems characterized by fine/coarse sandy beaches. Moreover, the numerical model performs well at sites characterized by gravelly beaches, highlighting its adaptability to a broader range of environmental conditions than those tested and recommended for the XBeach 2DH model.

CRediT authorship contribution statement

Samanta Buttò: Writing – original draft, Formal analysis, Data curation, Conceptualization. **Carla Lucia Faraci:** Writing – review & editing, Formal analysis, Conceptualization. **Marta Corradino:** Writing – review & editing, Conceptualization. **Claudio Iuppa:** Writing – review & editing, Formal analysis. **Emanuele Colica:** Writing – review & editing, Data curation. **Fabrizio Pepe:** Writing – review & editing, Conceptualization.

Declaration of competing interest

The authors declare that they have no known competing financial interests or personal relationships that could have appeared to influence the work reported in this paper.

Data availability

Datasets related to this article can be found at: https://www.dropbox.com/scl/fo/hxrdaqmrfqvxod6gm0jq0/AApDa-iqLlgrgAf8HYFvwto?rlkey=y0brg6r2rqzlbe24oref778ll&st=ml2suxjo&dl=0

Acknowledgements

We would like to thank the "Research & Planning Unit, Public Works Department, Ministry for Public Works and Planning" of Malta for providing essential survey tools. Christopher Gauci, Daniel Fenech and Jeremie Tranchant are acknowledged for their assistance in data collection. We also acknowledge the University of Malta and Prof. Sebastiano D'Amico for providing survey tools and logistic support.

Appendix A. Supplementary data

Supplementary data to this article can be found online at https://doi.org/10.1016/j.margeo.2024.107471.

References

Bailard, J.A., 1981. An energetics total load sediment transport model for a plane sloping beach. J. Geophys. Res. Oceans 86 (C11), 10938–10954. https://doi.org/10.1029/JC086iC11p10938.

Barbariol, F., Davison, S., Falcieri, F.M., Ferretti, R., Ricchi, A., Sclavo, M., Benetazzo, A., 2021. Wind waves in the Mediterranean Sea: an ERA5 reanalysis wind-based climatology. Front. Mar. Sci. 8 (November), 1–23. https://doi.org/10.3389/fmars.2021.760614.

Bayram, A., Larson, M., Hanson, H., 2007. A new formula for the total longshore sediment transport rate. Coast. Eng. 54 (9), 700–710. https://doi.org/10.1016/j.coastaleng.2007.04.001.

Bergillos, R.J., Masselink, G., Ortega-Sánchez, M., 2017. Coupling cross-shore and longshore sediment transport to model storm response along a mixed sand-gravel coast under varying wave directions. Coast. Eng. 129 (July), 93–104. https://doi.org/10.1016/j.coastaleng.2017.09.009.

Blott, S.J., Pye, K., 2001. GRADISTAT: a grain size distribution and statistics package for the analysis of unconsolidated sediments. Earth Surf. Process. Landf. 26, 1237–1248.

Boccotti, P., 1997. Idraulica Marittima. UTET.

Bodge, K.R., Kraus, N.C., 1991. Critical examination of longshore transport rate magnitude. Coast. Sedim. 139–155.

Booij, N., Holthuijsen, L.H., Ris, R.C., 1996. The "Swan" wave model for shallow water. In: Coastal Engineering, pp. 668–676. https://doi.org/10.1061/9780784402429.053.

Borg, J.A., Attrill, M.J., Rowden, A.A., Schembri, P.J., Jones, M.B., 2005. Architectural characteristics of two bed types of the seagrass *Posidonia oceanica* over different spatial scales. Estuar. Coast. Shelf Sci. 62 (4), 667–678. https://doi.org/10.1016/j.ecss.2004.10.003.

Bugajny, N., Furmańczyk, K., Dudzińska-Nowak, J., Paplińska-Swerpel, B., 2013. Modelling morphological changes of beach and dune induced by storm on the Southern Baltic coast using XBeach (case study: Dziwnow Spit). J. Coast. Res. 65 (January), 672–677. https://doi.org/10.2112/si65-114.1.

Caloiero, T., Aristodemo, F., Ferraro, D.A., 2022. Annual and seasonal trend detection of significant wave height, energy period and wave power in the Mediterranean Sea. Ocean Eng. 243 (October 2021), 110322. https://doi.org/10.1016/j.oceaneng.2021.110322.

Cartier, A., Héquette, A., 2015. Vertical distribution of longshore sediment transport on barred macrotidal beaches, northern France. Cont. Shelf Res. 93, 1–16. https://doi.org/10.1016/j.csr.2014.11.009.

CERC, 1984. Shore Protection Manual (Vols. 1–2). Dept. of the Army, U.S. Army Corps of Engineers, Coastal Engineering Research Center, Washington D.C.

Dabees, M., Kamphuis, J.W., 1998. ONELINE, a numerical model for shoreline change. Proc. Coast. Eng. Conf. 3, 2668–2681. https://doi.org/10.1061/9780784404119.202.

Dally, W.R., Dean, R.G., 1984. Suspended sediment transport and beach profile evolution. J. Waterw. Port Coast. Ocean Eng. 110 (1), 15–33. https://doi.org/10.1061/(asce)0733-950x(1984)110:1(15).

Dehouck, A., Dupuis, H., Sénéchal, N., 2009. Pocket beach hydrodynamics: the example of four macrotidal beaches, Brittany, France. Mar. Geol. 266 (1–4), 1–17. https://doi.org/10.1016/j.margeo.2009.07.008.

del Valle, R., Medina, R., Losada, M.A., 1993. Dependence of coefficient K on grain size. J. Waterw. Port Coast. Ocean Eng. 119 (5), 568–574.

DHI, 2005. MIKE 21/3 flow model FM hydrodynamic and transport module scientific documentation. In: DHI Group Horshølm.

Dolique, F., Anthony, E.J., 2005. Short-term profile changes of sandy pocket beaches affected by amazon-derived mud, Cayenne, French Guiana. J. Coast. Res. 21 (6), 1195–1202. https://doi.org/10.2112/04-0297.1.

Drago, A.F., Azzopardi, J., Gauci, A., Bruschi, A., Bruschi, A., 2013. Assessing the offshore wave energy potential for the Maltese Islands. In: ISE Annual Conference.

Elsayed, S.M., Oumeraci, H., 2017. Effect of beach slope and grain-stabilization on coastal sediment transport: an attempt to overcome the erosion overestimation by XBeach. Coast. Eng. 121 (December 2016), 179–196. https://doi.org/10.1016/j.coastaleng.2016.12.009.

Eversole, D., Fletcher, C.H., 2003. Longshore sediment transport rates on a reef-fronted beach: Field data and empirical models Kaanapali Beach, Hawaii. J. Coast. Res. 19 (3), 649–663.

Folk, R.L., Ward, W., 1957. Brazos river bar: a study in the significance of grain size parameters. J. Sediment. Petrol. 27 (1), 3–26.

Galappatti, G., Vreugdenhil, C.B., 1985. A depth-integrated model for suspended sediment transport. J. Hydraul. Res. 23 (4), 359–377. https://doi.org/10.1080/00221688509499345.

Galdies, C., 2011. The Climate of Malta: Statistics, Trends and Analysis 1951–2010 (Issue August 2011).

Garzon, J.L., Ferreira, Ó., Plomaritis, T.A., 2022. Modeling of coastal erosion in exposed and groin-protected steep beaches. J. Waterw. Port Coast. Ocean Eng. 148 (6), 1–16. https://doi.org/10.1061/(asce)ww.1943-5460.0000719.

Gatt, P., 2021. Embayment morphometrics, granulometry and carbonate mineralogy of sandy beaches in the Maltese Islands. Mar. Geol. 432 (June 2020), 106394. https://doi.org/10.1016/j.margeo.2020.106394.

Gessler, D., Hall, B., Spasojevic, M., Holly, F., Pourtaheri, H., Raphelt, N., 1999. Application of 3D mobile bed, hydrodynamic model. J. Hydraul. Eng. 125 (7), 737–749.

González, M., Medina, R., Gonzalez-Ondina, J., Osorio, A., Méndez, F.J., García, E., 2007. An integrated coastal modeling system for analyzing beach processes and beach restoration projects. SMC Comput. Geosci. 33 (7), 916–931. https://doi.org/10.1016/j.cageo.2006.12.005.

Haas, K.A., Hanes, D.M., 2004. Process based modeling of total longshore sediment transport. J. Coast. Res. 20 (3), 853–861. https://doi.org/10.2112/1551-5036(2004)20[853:pbmotl]2.0.co;2.

Hallermeier, R., 1981. A profile zonation for seasonal sand beaches from wave climate. Coast. Eng. 4, 253–277.

Hanson, H., 1989. Genesis: a generalized shoreline change numerical model. J. Coast. Res. 5 (1), 1–27. http://www.jstor.org/stable/4297483.

Hedegaard, I.B., Deigaard, R., Fredsøe, J., 1991. Onshore/offshore sediment transport and morphological modelling of coastal profiles. Coast. Sedim. 643–657.

Hwang, B., Do, K., Chang, S., 2024. Morphological changes in storm Hinnamnor and the Numerical Modeling of Overwash. J. Mar. Sci. Eng. 12 (1). https://doi.org/10.3390/jmse12010196.

Hydraulics, W., 1994. UNIBEST, A software suite for the simulation of sediment transport processes and related morphodynamics of beach profiles and coastline evolution. In: Programme Manual. WL|Delft Hydraulics, Delft, The Netherlands.
Jin, H., Do, K., Shin, S., Cox, D., 2021. Process-based model prediction of coastal dune erosion through parametric calibration. J. Mar. Sci. Eng. 9 (6). https://doi.org/10.3390/jmse9060635.
Kamphuis, J.W., 1991. Alongshore sediment transport rate distribution. J. Waterw. Port Coast. Ocean Eng. 117 (6), 624–640.
King, E.V., Conley, D.C., Masselink, G., Leonardi, N., McCarroll, R.J., Scott, T., Valiente, N.G., 2021. Wave, tide and topographical controls on headland sand bypassing. J. Geophys. Res. Oceans 126 (8). https://doi.org/10.1029/2020JC017053.
Korres, G., Oikonomou, C., Denaxa, D., Sotiropoulou, M., 2023. Mediterranean Sea waves analysis and forecast (copernicus marine service MED-waves, MEDWAM4 system) (version 1) [data set]. Copernicus Monitor. Environ. Mar. Service. https://doi.org/10.25423/CMCC/MEDSEA_ANALYSISFORECAST_WAV_006_017_MEDWAM4.
Kraus, N.C., 1987. Rates in the Surf Zone Measurements of Sediment Transport Rate, 3, pp. 139–152.
Larson, M., Hoan, L.X., Hanson, H., 2010. Direct formula to compute wave height and angle at incipient breaking. J. Waterw. Port Coast. Ocean Eng. 136 (2), 119–122. https://doi.org/10.1061/(asce)ww.1943-5460.0000030.
Le Hir, P., Monbet, Y., Orvain, F., 2007. Sediment erodability in sediment transport modelling: can we account for biota effects? Cont. Shelf Res. 27 (8), 1116–1142. https://doi.org/10.1016/j.csr.2005.11.016.
Lesser, G.R., Roelvink, J.A., van Kester, J.A.T.M., Stelling, G.S., 2004. Development and validation of a three-dimensional morphological model. Coast. Eng. 51 (8–9), 883–915. https://doi.org/10.1016/j.coastaleng.2004.07.014.
Malta Maritime Authority (MMA), 2003. Malta Significant Wave Height Study: Main Report.
Masselink, G., Russell, P., Turner, I., Blenkinsopp, C., 2009. Net sediment transport and morphological change in the swash zone of a high-energy sandy beach from swash event to tidal cycle time scales. Mar. Geol. 267 (1–2), 18–35. https://doi.org/10.1016/j.margeo.2009.09.003.
McCall, R.T., Thiel, Van, de Vries, J.S.M., Plant, N.G., Van Dongeren, A.R., Roelvink, J. A., Thompson, D.M., Reniers, A.J.H.M., 2010. Two-dimensional time dependent hurricane overwash and erosion modeling at Santa Rosa Island. Coast. Eng. 57 (7), 668–683. https://doi.org/10.1016/j.coastaleng.2010.02.006.
Mil-Homens, J., Ranasinghe, R., van Thiel de Vries, J.S.M., Stive, M.J.F., 2013. Re-evaluation and improvement of three commonly used bulk longshore sediment transport formulas. Coast. Eng. 75, 29–39. https://doi.org/10.1016/j.coastaleng.2013.01.004.
Pereira Quadrado, G., Goulart, E.S., 2020. Longshore sediment transport: predicting rates in dissipative sandy beaches at southern Brazil. SN Appl. Sci. 2 (6), 23–33. https://doi.org/10.1007/s42452-020-03223-x.
Rattanapitikon, W., Shibayama, T., 2006. Breaking wave formulas for breaking depth and orbital to phase velocity ratio. Coast. Eng. J. 48 (4), 395–416. https://doi.org/10.1142/S0578563406001489.
Robertson, B., Hall, K., Zytner, R., NISTOR, I., 2013. Breaking waves: review of characteristic relationships. Coast. Eng. J. 55 (1), 1350002. https://doi.org/10.1142/S0578563413500022.
Roelvink, J.A., Stive, M.F.J., 1989. Bar-generating cross-shore flow mechanisms on a beach. In. J. Geophys. Res. 94 (C4), 4785–4800. https://doi.org/10.1029/JC094iC04p04785.
Roelvink, D., Reniers, A., van Dongeren, A., van Thiel de Vries, J., McCall, R., Lescinski, J., 2009. Modelling storm impacts on beaches, dunes and barrier islands. Coast. Eng. 56 (11−12), 1133–1152. https://doi.org/10.1016/j.coastaleng.2009.08.006.
Roelvink, D., Reniers, A., Van Dongeren, A.P., Van Thiel de Vries, J., Lescinski, J., McCall, R., 2010. XBeach model description and manual. In: Unesco-IHE Institute for Water Education, Deltares and Delft University of Tecnhology. Report June, 21, 2010.
Roelvink, D., McCall, R., Mehvar, S., Nederhoff, K., Dastgheib, A., 2018. Improving predictions of swash dynamics in XBeach: the role of groupiness and incident-band runup. Coast. Eng. 134 (February 2017), 103–123. https://doi.org/10.1016/j.coastaleng.2017.07.004.
Rosati, J.D., 2005. Concepts in sediment budgets. J. Coast. Res. 21 (2), 307–322. https://doi.org/10.2112/02-475A.1.
Rosati, J., Walton, T.L., Bodge, K., 2002. Longshore sediment transport. In: Coastal Engineering Manual, Part III-2. Army Corps of Engineers, Washington, DC (engineer manual 1110-2-1100 edition).
Salem Cherif, Y., Mezouar, K., Guerfi, M., Sallaye, M., Dahmani, A.E.A., 2019. Nearshore hydrodynamics and sediment transport processes along the sandy coast of Boumerdes, Algeria. Arab. J. Geosci. 12 (24). https://doi.org/10.1007/s12517-019-4981-0.
Samaras, A.G., Koutitas, C.G., 2014. Comparison of three longshore sediment transport rate formulae in shoreline evolution modeling near stream mouths. Ocean Eng. 92, 255–266. https://doi.org/10.1016/j.oceaneng.2014.10.005.
Sanil Kumar, V., Anand, N.M., Chandramohan, P., Naik, G.N., 2003. Longshore sediment transport rate - measurement and estimation, central west coast of India. Coast. Eng. 48 (2), 95–109. https://doi.org/10.1016/S0378-3839(02)00172-2.
Satheeshkumar, J., Balaji, R., 2021. Field measurement and modeling of sediment transport along a Sandy Pocket Beach, Central West Coast of India. J. Waterw. Port Coast. Ocean Eng. 147 (6), 5021014. https://doi.org/10.1061/(ASCE)WW.1943-5460.0000678.
Schoonees, J.S., Theron, A.K., 1993. Review of the field-data base for longshore sediment transport. Coast. Eng. 19 (1–2), 1–25. https://doi.org/10.1016/0378-3839(93)90017-3.
Shanas, P.R., Sanil Kumar, V., 2014. Coastal processes and longshore sediment transport along Kundapura coast, central west coast of India. Geomorphology 214, 436–451. https://doi.org/10.1016/j.geomorph.2014.02.027.
Simmons, J.A., Splinter, K.D., 2022. A multi-model ensemble approach to coastal storm erosion prediction. Environ. Model. Softw. 150. https://doi.org/10.1016/j.envsoft.2022.105356.
Simmons, J.A., Splinter, K.D., Harley, M.D., Turner, I.L., 2019. Calibration data requirements for modelling subaerial beach storm erosion. Coast. Eng. 152 (November 2018), 103507. https://doi.org/10.1016/j.coastaleng.2019.103507.
Soukissian, T., Karathanasi, F., Axaopoulos, P., Voukouvalas, E., Kotroni, V., 2018. Offshore wind climate analysis and variability in the Mediterranean Sea. Int. J. Climatol. 38 (1), 384–402. https://doi.org/10.1002/joc.5182.
Sperati, S., Alessandrini, S., D'Amico, F., Cheng, W., Rozoff, C.M., Bonanno, R., Lacavalla, M., Aiello, M., Airoldi, D., Amaranto, A., Decimi, G., Vergata, M.A., 2024. A new Wind Atlas to support the expansion of the Italian wind power fleet. Wind Energy 27 (3), 298–316. https://doi.org/10.1002/we.2890.
Tassi, P., Benson, T., Delinares, M., Fontaine, J., Huybrechts, N., Kopmann, R., Pavan, S., Pham, C.T., Taccone, F., Walther, R., 2023. GAIA - a unified framework for sediment transport and bed evolution in rivers, coastal seas and transitional waters in the TELEMAC-MASCARET modelling system. Environ. Model. Softw. 159 (September 2022), 105544. https://doi.org/10.1016/j.envsoft.2022.105544.
Tomasicchio, G.R., Lamberti, A., Guiducci, F., 1994. Stone movement on a reshaped profile. In: Proceedings of the Coastal Engineering Conference (Vol. 2), pp. 1625–1640. https://doi.org/10.1061/9780784400890.118.
Tomasicchio, Giuseppe R., D'Alessandro, F., Barbaro, G., Malara, G., 2013. General longshore transport model. Coast. Eng. 71, 28–36. https://doi.org/10.1016/j.coastaleng.2012.07.004.
Tomasicchio, Giuseppe Roberto, D'Alessandro, F., Barbaro, G., Ciardulli, F., Francone, A., Mahmoudi Kurdistani, S., 2017. General model for estimation of longshore transport at shingle/mixed beaches. Coast. Eng. Proc. 35, 26. https://doi.org/10.9753/icce.v35.sediment.26.
Van Rijn, L.C., 1993. Principles of Sediment Transport in Rivers, Estuaries and Coastal Seas. International Institute for Infrastructural, Hydraulic, and Environmental Engineering, Delft, The Netherlands.
Van Rijn, L.C., 2003. Longshore Sand Transport Leo C. van Rijn 1. 28th ICCE, Cardiff, UK, pp. 1–13.
Van Rijn, L.C., 2014. A simple general expression for longshore transport of sand, gravel and shingle. Coast. Eng. 90, 23–39. https://doi.org/10.1016/j.coastaleng.2014.04.008.
Van Wellen, E., Chadwick, A.J., Mason, T., 2000. A review and assessment of longshore sediment transport equations for coarse-grained beaches. Coast. Eng. 40 (3), 243–275. https://doi.org/10.1016/S0378-3839(00)00031-4.
Walton, T.L., Bruno, R.O., Walton Jr., T.L., Bruno, R.O., 1989. Longshore transport at a detached breakwater, phase II. J. Coast. Res. 1982, 679–691.
Wang, P., Kraus, N.C., 1999. Longshore sediment transport rate measured by short-term impoundment. J. Waterw. Port Coast. Ocean Eng. 125 (3), 118–126.
Wang, P., Kraus, N.C., Davis, R.A., 1998. Total longshore sediment transport rate in the surf zone: Field measurements and empirical predictions. J. Coast. Res. 14 (1), 269–282.
Wang, P., Smith, E.R., Ebersole, B.A., 2002. Large-scale laboratory measurements of longshore sediment transport under spilling and plunging breakers. J. Coast. Res. 18 (1), 118–135.
Widdows, J., Brinsley, M., 2002. Impact of biotic and abiotic processes on sediment dynamics and the consequences to the structure and functioning of the intertidal zone. J. Sea Res. 48 (2), 143–156. https://doi.org/10.1016/S1385-1101(02)00148-X.
Williams, J.J., Esteves, L.S., Lisniowski, M.A., 2008. Towards improving the prediction of longshore sediment transport. IAHS-AISH Publ. 325, 599–606.
XBeach manual: Release XBeach 1.24.6057 Halloween. *Https://Xbeach.Readthedocs.Io/En/Latest/Index.Html*, 2023.